

Charge transfer between $\text{ND}_3^+(\nu_2^+)$ and phenol

Ho-Tae Kim, Richard J. Green, and Scott L. Anderson

Department of Chemistry, University of Utah, 315 South 1400 East RM Dock, Salt Lake City, Utah 84112-0850

(Received 1 June 2000; accepted 21 June 2000)

Reactions of vibrationally state-selected ND_3^+ with phenol were studied in a guided beam arrangement. There are four exoergic channels, of which only charge transfer (CT) has significant intensity. The dominant mechanism requires intimate collisions, with little long-range electron hopping. Despite the presence of deep hydrogen-bonded wells, only a few percent of collisions form long-lived complexes. ND_3^+ vibration has no effect on CT at low energies, with weak inhibition at high energies. Charge transfer with H/D exchange is a minor channel, inhibited by ND_3^+ vibration and collision energy. The small vibrational effects are in contrast to the large effects observed in reaction of $\text{PhOH}^+(\nu_{6a}, \nu_{12})$ with ND_3 . © 2000 American Institute of Physics. [S0021-9606(00)01035-7]

I. INTRODUCTION

We have found that measurements of the effects of reactant vibrational excitation and collision energy, together with product recoil velocity distributions, provide a powerful tool for unraveling reaction dynamics in relatively complex systems. We report here a study of the reaction of $\text{ND}_3^+(\nu_2^+=0,3,5)$ with phenol—a prototypical system for the study of atom and charge transfer reactions mediated by hydrogen-bonded complexes. The energetics for the $[\text{ND}_3:\text{PhOH}]^+$ system are shown in Fig. 1. The binding energies of the complexes are taken from our QCISD(T)/6-31G* calculations¹ and the product energetics were calculated using thermochemical data in the literature.²⁻⁴ As shown, there are two hydrogen-bonded complexes, interconverting by intracomplex proton transfer. The calculated barrier to interconversion depends on the level of theory, but is clearly small compared to the available energy. There are also two ring-bound complexes in which the ND_3 is coordinated, via its lone pair orbital, at ortho and para positions on the PhOH ring. There appears to be a significant barrier separating the ring and hydrogen-bonded geometries, although still well below the energy of separated $\text{ND}_3^+ + \text{PhOH}$ reactants. There are also four distinct product channels with substantial exoergicity. The two lowest energy channels are charge transfer (CT) and CT with H/D exchange (CT/X). Next is hydrogen abstraction (HA) producing $\text{ND}_3\text{H}^+ + \text{PhO}$, and highest is proton transfer (PT), producing $\text{PhOHD}^+ + \text{ND}_2$.

We recently reported¹ a study of the reaction of PhOH^+ with ND_3 , i.e., the same reactive system, $[\text{ND}_3:\text{PhOH}]^+$, but starting in the lower energy reactant charge state. In that reaction, both ring-bound and hydrogen-bonded complexes are important intermediates, and two major product channels are observed: $\text{PhOD}^+ + \text{ND}_2\text{H}$; and $\text{PhO} + \text{ND}_3\text{H}^+$. There was also significant dissociation of the intermediate complexes back to $\text{PhOH}^+ + \text{ND}_3$ reactants. These exit channels correspond to the CT/X, HA, and CT channels in Fig. 1, respectively. Perhaps the most interesting and surprising re-

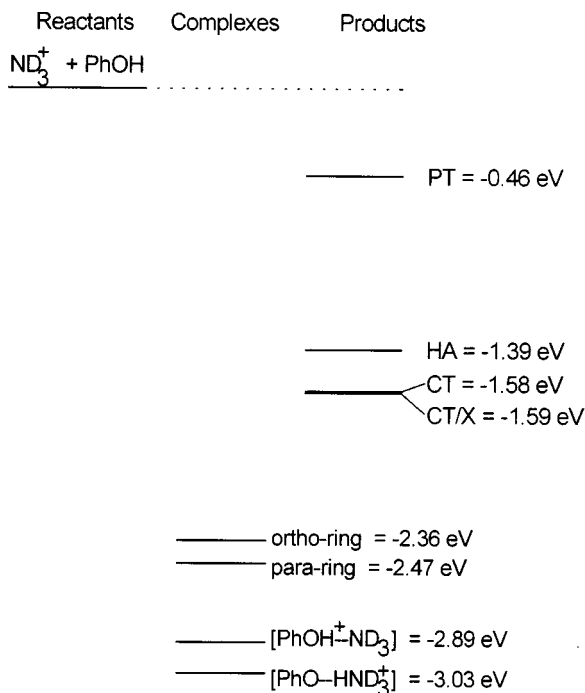
sult of that study was that excitation of low-frequency, in-plane ring modes (ν_{6a} and ν_{12}) of PhOH^+ substantially affected the chemistry. For example, the $\text{PhOD}^+ + \text{ND}_2\text{H}$ channel was enhanced by over a factor of two, even though there is no obvious connection between the vibrational motion and the reaction coordinate for this H/D exchange reaction. The explanation proposed was that the ring vibrations promote isomerization from ring-bound to hydrogen-bonded complexes, allowing the ring-bound complexes to serve as precursors for hydrogen bond formation. The principle motivation of the present study was to examine the effects of ND_3^+ vibrational excitation on the analogous reactions in $\text{ND}_3^+ + \text{PhOH}$.

II. EXPERIMENT

The experimental and analysis methodologies have been described previously.^{5,6} Briefly, ND_3^+ with variable excitation in the ν_2^+ umbrella vibration was generated by REMPI through the *B* and *C* intermediate states.^{7,8} The ions are formed into a beam with narrow temporal and velocity distributions (15 μsec and 300 m/sec, respectively), then injected into an octapole ion guide, that guides them through a scattering cell containing 6×10^{-5} Torr of PhOH vapor. Product ions, together with unreacted ND_3^+ , are collected by the octapole, then transferred into a second, longer octapole where their velocities can be measured by time-of-flight (TOF). TOF is also used to calibrate the collision energy scale. Finally, ions are mass-analyzed and counted by a multichannel scalar. We verified that reaction was occurring under single collision conditions by measuring over a range of scattering cell pressures, to see that the cross sections are pressure-independent.

III. RESULTS

The cross sections for all product channels with measurable intensity are shown in Fig. 2, for ND_3^+ in its ground state and with $\nu_2^+=3$ and 5 excitation. Only the two charge transfer channels are observed:

FIG. 1. Energetics for the $[\text{ND}_3:\text{PhOH}]^+$ system.

$$\Delta H = -1.58 \text{ eV},$$



$$\Delta H = -1.59 \text{ eV}.$$

For comparison, the collision cross section is plotted as a heavy solid line. $\sigma_{\text{collision}}$ is taken as the greater of the hard sphere cross section ($\sim 63 \text{ \AA}^2$) or capture cross section, calculated using the statistical adiabatic channel theory of Troe.⁹ The measured charge transfer efficiency ($\sigma_{\text{CT}}/\sigma_{\text{collision}}$) is $\sim 70\%$ at low energies, declining to 40% by 2 eV.

The kinematics in this system are such that at low collision energies, the velocity of the center-of-mass in the lab frame (V_{CM}) is only a few hundred m/s, thus back-scattered product ions have low, or even negative velocities in the lab frame. To collect these slow or back-scattered ions, the ion lens used to inject ions into the scattering octapole is biased a few tenths of a volt positive with respect to the octapole, so as to reflect back-scattered ions. In addition, we bias the second octapole 1.5 volts negative with respect to the scattering octapole, to help extract and transmit slow product ions. Nonetheless, there can be small potential barriers in the scattering octapole that can reduce detection efficiency for slow ions. As these barriers vary from day to day, we find that the cross section at low energies has higher-than-usual uncertainty. The cross sections reported are averages of at least several runs on different days, and the repeatability ranges from $\pm 8 \text{ \AA}^2$ at $E_{\text{collision}} = 0.3 \text{ eV}$, to $\pm 2 \text{ \AA}^2$ at 2 eV, corresponding to about $\pm 10\%$ over the entire energy range. Because all cross sections were measured under identical conditions, the repeatability is a reasonable estimate for the error in comparing cross sections for different vibrational

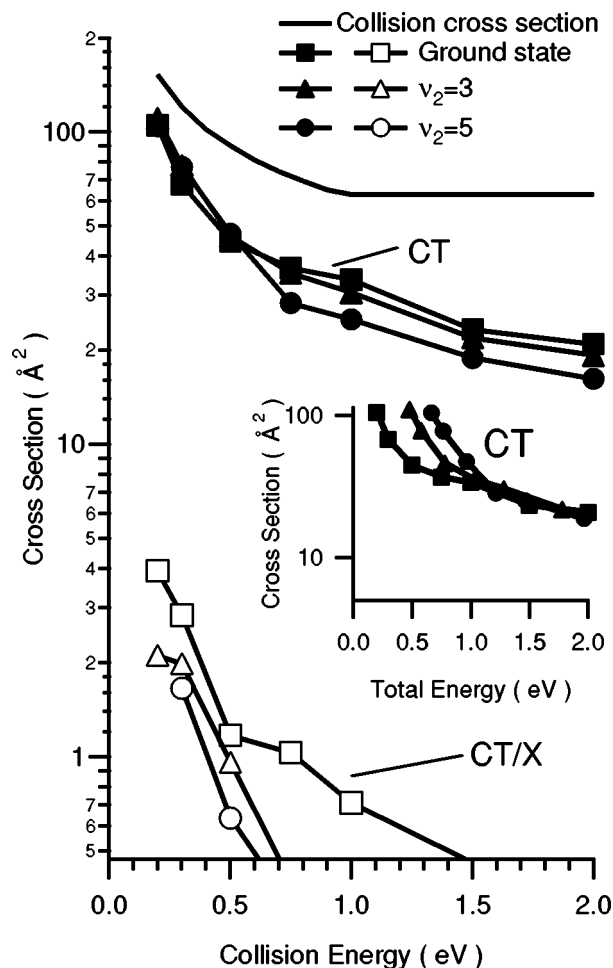


FIG. 2. Cross sections for charge transfer (CT: filled symbols) and charge transfer with H/D exchange (CT/X: open symbols) as a function of collision energy and ND_3^+ vibrational state. Also shown is the collision cross section (see text). Main figure: cross sections vs collision energy. Inset: CT cross sections vs total energy.

states. Because it is likely that we lose some slow ions, however, the absolute cross section at low collision energies should be regarded as a lower limit.

Note that the CT/X product ion has the same mass (95) as the CT product with one ^{13}C substitution. At high collision energies the mass 95 signal is, within the uncertainty, just 6.67% of the mass 94 signal, as expected if this channel were entirely due to ^{13}C contamination (1.1% ^{13}C abundance). At low energies the 95 signal is about 12% of the CT signal, indicating real CT/X product. The cross section plotted in Fig. 2 has been corrected for the ^{13}C contribution. One surprise was that no signal is observed for the hydrogen abstraction channel, even though this channel is only slightly less exoergic than CT. Note that in reaction of the $\text{PhOH}^+ + \text{ND}_3$ charge state, the analogous product is observed, even though the reaction is endoergic for that charge state. No signal is observed for the PT reaction, either, presumably reflecting the fact that PT is substantially less energetically favorable.

There are two ways of looking at the vibrational effects. When plotted versus collision energy, there is no effect of vibration on the CT reaction at low energies and weak inhibition at high energies. Another common way of plotting vibrational effects is to compare cross sections for different reactant states as a function of total energy. As shown in the inset to Fig. 2, partitioning energy from collision energy to vibration leads to substantial increases in apparent CT reactivity at low total energies. This “effect” really has nothing to do with vibration. Rather, it originates entirely from the increase in σ_{capture} attendant on decreasing collision energy. Note that the inhibition at high collision energies disappears when plotted against total energy, indicating that energy in ND_3^+ vibration and collision energy have similar effects at high energies. For the CT/X reaction, the small cross section and ^{13}C subtraction process increase the experimental uncertainty. Nonetheless, there is clearly significant vibrational inhibition of the CT/X channel.

Measurements of velocity distributions for the product ions usually provide considerable additional dynamical insight. Two pieces of information can be inferred from such distributions. If reaction proceeds via a collision intermediate with lifetime long compared to its rotational period, the resulting axial velocity distributions must be forward-backward symmetric with respect to V_{CM} . Conversely, an asymmetric distribution implies a direct reaction where the collision time is short, and allows the preferred scattering direction to be determined. In addition, the maximum deviation of the velocity distribution from V_{CM} is a measure of the maximum energy going into recoil of the products.

As noted, the kinematics in this system are such for low collision energies, a large fraction of the range of possible product ion velocities is at small or negative lab velocities. The negative part of the velocity distribution cannot be directly measured in our configuration, and the velocities of slow ions are easily distorted by surface potentials on the octapole. We estimate that the minimum reliably-measured lab velocity is about 500 m/sec for this system. At low energies, V_{CM} is below 500 m/s, and only the forward-scattered tail of the velocity distribution can be measured. Only at the highest energies is V_{CM} large enough to allow measurement of a significant fraction of the backward-scattered part of the velocity distribution. At $E_{\text{collision}}=2$ eV, the distribution is clearly backward-peaked, although quite broad and extending well into the forward hemisphere. (We define “forward” as product ions with velocities in the direction of the initial ion motion.) We have not attempted to fit the distribution, as there is still a significant velocity range that is missed. No useful information can be extracted for the low energy CT or CT/X channels.

RRKM calculations of complex lifetimes and product branching ratios were performed to aid interpretation. We used the RRKM program of Zhu and Hase,¹⁰ with its direct state count algorithm, and our *ab initio* frequencies and energetics. The calculations assume orbiting transition states^{11–13} for dissociation of the complexes, and were done for complexes with angular momentum equal to the average L leading to capture in the statistical adiabatic channel model. Recall that the reactant charge state lies 1.58 eV

TABLE I. RRKM lifetimes and branching ratios.

$E_{\text{collision}}$ (eV)	Hydrogen-bonded lifetime (fsec)	Direct collision time (fsec)
0.2	520	65
0.5	240	41
1.0	<100 ^a	30
2.0	<100	21

^aLifetime below the range required for the energy randomization assumed in RRKM theory.

above the $\text{PhOH}^+ + \text{ND}_3$ products, so that even at our lowest collision energies, the available energy is about twice the complex binding energy. The RRKM results are summarized in Table I. To give some idea how the lifetimes compare to the time scale for direct scattering, we also give a “direct collision time,” defined arbitrarily as the time required for relative motion by 1 Å. Note that the lifetime of the hydrogen-bonded complex is significantly longer than the direct collision time for low energies, but probably mechanically insignificant at high energies. Lifetimes are not given for the more weakly bound, ring-coordination complexes, as they are too short to be mechanically significant at all collision energies.

IV. DISCUSSION

For a system like this, with deep potential wells that might stabilize intermediate complexes, there are several charge transfer mechanisms that may contribute. At one extreme is capture into a complex, from which CT and CT/X products are possible dissociation channels. The other extreme is long-range charge transfer, where the charge is transferred at large intermolecular separations, at which point the intermolecular interaction is weak. Note that long-range CT can occur both in large impact parameter collisions, where the reactants never come into intimate contact, and during the approach or separation phases of more intimate collisions. Because the probability of collisions at given impact parameter (b) is proportional to b , the collision cross section is dominated by large b collisions. As a consequence, in systems where long-range CT is efficient, it is the dominant mechanism, and the CT cross section is generally quite large—sometimes in excess of the hard sphere cross section.

The factor controlling the efficiency of long-range CT is conservation of energy, i.e., the requirement that the CT exoergicity must somehow be converted to other forms of energy in the products. At long-range, intermolecular forces are too weak to allow significant coupling into recoil energy of the products, and there are no impulsive forces that might excite product vibrational states. As a consequence, long-range CT is only efficient if there are product states that are near-resonant with, and which have substantial wave function overlap with the reactant state (i.e., large Franck-Condon factors). If such states do not exist, then intimate collisions are required to distribute the CT exoergicity into product degrees of freedom.

Because there can be little momentum transfer in large impact parameter collisions, the clearest signature of efficient

long-range CT is product ions that are very slow in the lab frame, i.e., sharply back-scattered in the center-of-mass frame. (Long-range CT could also occur in small b collisions where momentum transfer is efficient, however, large b collisions will always dominate.) CT mediated by a long-lived complex will give product velocity distributions that are forward-backward symmetric with respect to V_{CM} , typically with little energy partitioned into recoil. The intermediate case, CT occurring by impulsive short-lived collisions, typically gives broad angular and energy distributions, with the details depending on the range of impact parameters leading to CT.⁶

The observation of an asymmetric velocity distribution at high collision energies indicates that CT is dominated by collisions with time scales shorter than the rotational period of the collision complex (~ 1.8 psec).¹ This result is certainly consistent with the negligible RRKM lifetime calculated at high energies. The velocity distribution is back-scattered, however it is very broad, and extends well into the forward direction. The broad distribution indicates considerable momentum transfer, ruling out dominance by a long-range CT mechanism. High energy CT appears to occur over a wide range of impact parameters, with low impact parameters leading to forward-scattered product ions, and larger impact parameters leading to sideways or back-scattered product ions.

The absence of long-range CT is probably a consequence of the large CT exoergicity. In a long-range mechanism, the exoergicity (1.58 eV) must go primarily into vibrations of the products. PhOH does not undergo a large geometry change upon ionization, and as a consequence there are few Franck-Condon-active vibrations. For example, the He I photoelectron spectrum of PhOH is narrow, with only a small probability for more than ~ 0.3 eV of vibrational excitation.¹⁴ Because ND_3^+ undergoes a planar-to-pyramidal transition upon neutralization, its ν_2 umbrella bend vibration is strongly Franck-Condon active. Ebata *et al.*¹⁵ have calculated ν_2 level energies and Franck-Condon factors for $\text{ND}_3^+(\nu_2^+) \rightleftharpoons \text{ND}_3(\nu_2)$ transitions with ν_2^+ and ν_2 up to 8. Starting with $\text{ND}_3^+(\nu_2^+ = 0)$, if only half the CT exoergicity must go into ν_2 , this corresponds to $\text{ND}_3(\nu_2 = 8)$, and the Franck-Condon factor is only 0.003.

For large reactant molecules, long-range CT may be of limited significance for geometric reasons. CT cannot occur until the interreactant separation is small enough (typically a few angstroms) to give a significant matrix element coupling the two charge states. Long-range CT occurs only for that range of impact parameters where trajectories reach this critical separation, but do not penetrate to shorter ranges where substantial momentum transfer occurs. For large molecules, the repulsive wall is at large separations, diminishing the relative importance of such collisions. Even so, for reactants the size of ND_3^+ and phenol, efficient long-range CT can significantly enhance the cross section. For example, if the critical separation for charge state mixing is just 2.5 \AA greater than the hard sphere separation, then efficient long-range CT would go with a cross section of $\sim 150 \text{ \AA}^2$, i.e., more than five times the observed cross section.

At lower energies, the hydrogen-bonded complex life-

time becomes mechanistically significant, and we have no recoil velocity information providing insight into collision time scales. The product branching ratios suggest, however, that CT continues to be dominated by collisions that do not trap into the hydrogen-bonded well. In our previous study of the $\text{PhOH}^+ + \text{ND}_3$ system,¹ we showed that H/D exchange occurs in the hydrogen-bonded complex, and that only the hydroxyl and ammonia hydrogen atoms are exchanged. We also reported RRKM rates for both intracomplex H/D exchange and for dissociation of the complex. Because three of the four exchanging atoms are deuterium, we would expect a substantial fraction of CT/X products at low collision energies, if CT occurred via a statistical, hydrogen-bonded complex. Instead, the CT/X cross section is only a few percent of the total, suggesting that more than 90% of CT does not involve a statistical complex formation, even at low collision energies. This conclusion is also consistent with nonobservation of HA products—another decay channel for the hydrogen-bonded complex.¹ It appears that in slow collisions that might be expected to trap into the hydrogen-bonded well, the 1.58 eV of electronic energy is released early in the collision, and is sufficient to cause dissociation to products before energy can be randomized.

In summary, the data suggest that CT takes place primarily in intimate collisions at all energies, and that the collision time scale remains short, except in the small fraction of low energy collisions where hydrogen-bonded complexes form. The cross section for CT, including CT/X, is substantially less than the collision cross section at high energies, corresponding to efficiency of only 40%. The efficiency is probably limited by the need to put high vibrational energies into the products. The axial velocity measurements indicate that the average product recoil energy is considerably less than the collision energy. Internal modes of the products must, therefore, accommodate both the exoergicity (1.58 eV) and a substantial fraction of the collision energy. Evidently, only $\sim 40\%$ of high energy collisions are able to accomplish the required E, T to V conversion. The inhibition observed from ν_2^+ excitation is consistent with this picture. The two vibrational states correspond to 0.27 and 0.46 eV, respectively, thus significantly increasing the total energy that must be accommodated in product vibration. As shown in the inset to Fig. 2, vibrational energy and collision energy have similar effects, suggesting that total energy is the determining factor.

It seems reasonable to attribute the increase in CT efficiency at low collision energies mostly to slower approach and impact, increasing the interaction time and the probability for the large energy redistributions required. There may also be an enhancement simply from the fact that there is less total energy in the reactants that must be partitioned to the products, however, the absence of vibrational inhibition at low energies suggests that collision energy, rather than total energy, is the determining factor in this energy range.

The vibrational inhibition observed for the CT/X channel is not surprising. Because this reaction involves H/D exchange, long collision times are required. Addition of significant amounts of reactant vibrational energy is expected to reduce the (already small) probability for forming a long-

lived complex, and also to shorten the lifetime. Even at our lowest collision energies, the RRKM lifetime of the hydrogen-bonded complex is comparable to the time scale for H/D exchange within the complex,¹ thus any shortening of lifetime will decrease the exchange probability.

V. CONCLUSION

Reaction of ND_3^+ with phenol is dominated by charge transfer, with undetectably small cross sections for the exoergic hydrogen abstraction or proton transfer reactions. Most CT goes via direct intimate collisions at all energies, and the efficiency of CT is reduced by the need to accommodate the large exoergicity. Vibrational effects are small, and can be rationalized in terms of the vibrational energy.

ACKNOWLEDGMENTS

This work was supported by the National Science Foundation under grant CHE-9807625. We are also grateful for a grant of computer time from the Utah Center for High Performance Computing. The SGI Origin 2000 used was funded in part by the SGI Supercomputing Visualization Center Grant.

- ¹R. J. Green, H.-T. Kim, J. Qian, and S. L. Anderson, *J. Chem. Phys.* **113**, 4158 (2000).
- ²S. G. Lias, J. E. Bartmess, J. F. Liebman, J. L. Holmes, R. D. Levin, and W. G. Mallard, in *NIST Chemistry WebBook, NIST Standard Reference Database Number 69*, edited by W. G. Mallard and P. J. Linstrom (National Institute of Standards and Technology, Gaithersburg, MD 20899, 2000) (<http://webbook.nist.gov>).
- ³S. G. Lias, J. E. Bartmess, J. F. Liebman, J. L. Holmes, and R. D. Levin, *J. Phys. Chem. Ref. Data* **17** (1988).
- ⁴H.-T. Kim, R. J. Green, J. Qian, and S. L. Anderson, *J. Chem. Phys.* **112**, 5717 (2000).
- ⁵Y.-h. Chiu, H. Fu, J.-t. Huang, and S. L. Anderson, *J. Chem. Phys.* **102**, 1199 (1995).
- ⁶Y.-h. Chiu, H. Fu, J.-t. Huang, and S. L. Anderson, *J. Chem. Phys.* **105**, 3089 (1996).
- ⁷W. E. Conaway, R. J. S. Morrison, and R. N. Zare, *Chem. Phys. Lett.* **113**, 429 (1985).
- ⁸H. Fu, J. Qian, R. J. Green, and S. L. Anderson, *J. Chem. Phys.* **108**, 2395 (1998).
- ⁹J. Troe, *Chem. Phys. Lett.* **122**, 425 (1985).
- ¹⁰L. Zhu and W. L. Hase, *Quant. Chem. Prog. Exchange*, QCPE program 644.
- ¹¹M. T. Rodgers, K. M. Ervin, and P. B. Armentrout, *J. Chem. Phys.* **106**, 4499 (1997).
- ¹²M. T. Rodgers and P. B. Armentrout, *J. Chem. Phys.* **109**, 1787 (1998).
- ¹³E. V. Waage and B. S. Rabinovitch, *Chem. Rev.* **70**, 377 (1970).
- ¹⁴K. Kimura, S. Katsumata, Y. Achiba, T. Yamazaki, and S. Iwata, *Handbook of HeI Photoelectron Spectra of Fundamental Organic Molecules* (Japan Scientific Societies, Tokyo, 1981).
- ¹⁵T. Ebata, W. E. Conaway, and R. N. Zare, *Int. J. Mass Spectrom. Ion Processes* **80**, 51 (1987).